Journal of Inorganic and Organometallic Polymers and Materials (2020) 30:1110–1120
https://doi.org/10.1007/s10904-019-01286-x

Synthesis of Novel Schiff Base Cobalt (II) and Iron (III) Complexes as Cathode Catalysts for Microbial Fuel Cell Applications

Pinar Sen[1] · Dilan Akagunduz[2] · Araz Sheibani Aghdam[3] · Fevzi Çakmak Cebeci[3] · Tebello Nyokong[1] · Tunc Catal[2,4]

Received: 7 May 2019 / Accepted: 16 August 2019 / Published online: 22 August 2019

Abstract
In this study, the synthesis and characterization of a new Schiff base and its cobalt(II) and iron(III) complexes were performed fully characterized by common spectroscopic techniques such as ^{1}H-NMR, ^{13}C-NMR, FT-IR, UV–Vis and MS and elemental analysis. The cathodes prepared with only activated carbon, Co-Schiff base complex, and Fe-Schiff base complex mixed with activated carbon as the carrier were examined in single chamber air cathode microbial fuel cells (MFCs). The spectroscopic results confirm the structure of novel Schiff base and its complexes with cobalt (II) and Fe(III). MFC results showed that Fe-Schiff base complex generated higher voltage generation using glucose as the carbon source. Cyclic voltammetry results showed the conductivity and catalytic features of the cathodes developed in this study. Scanning electron microscopic results showed the distribution the complexes on the cathode surface. In conclusion, a novel Schiff base and its complexes with cobalt (II) and iron (III) can be employed into MFC technology to be used in green electricity production, and might help decreasing the operating costs of wastewater treatment plants.

Keywords Cathode · Cyclic voltammetry · Electricity · Schiff base · Cobalt · Iron · Metal complex · Microbial fuel cell

1 Introduction

The Schiff bases have been used largely as versatile ligands in the area of coordination chemistry since they coordinate to metal ions through imine nitrogen to form stable complexes [1–4]. The most common Schiff bases have N_2O_2 donor atoms, which are called tetradentate bis-Schiff base ligands, and the produced Schiff bases describe the class of Salen-type [5–7].

✉ Tebello Nyokong
t.nyokong@ru.ac.za

✉ Tunc Catal
tunc.catal@uskudar.edu.tr

[1] Department of Chemistry, Institute for Nanotechnology Innovation, Rhodes University, PO Box 94, Grahamstown 6140, South Africa

[2] Istanbul Protein Research-Application and Inovation Center (PROMER), Uskudar University, Uskudar, 34662 Istanbul, Turkey

[3] Faculty of Engineering and Natural Sciences, Sabanci University, 34956 Istanbul, Turkey

[4] Department of Molecular Biology and Genetics, Uskudar University, Uskudar, 34662 Istanbul, Turkey

N_2O_2 donor ligands as the class that constitutes the structure of our study have been studied extensively for different applications due to their unique structural properties [8–10].

The complexation of Schiff bases with transition metals enabled them to be used in various fields with its easy preparation and structural diversity such as catalysis [11], electroluminescent materials [12], organic photovoltaic materials [13], in medicinal chemistry [14], in biological process as antibiotic, antiviral and antitumor agents [15], in non-linear optical devices [16].

The structural, physical and chemical properties of Schiff bases metal complexes are affected by the nature of the ligand structure [17]. Besides this, the choice of the appropriate metal center is crucial for intended applications. So far, many novel transition metal complexes of salen-type containing N_2O_2 donor atoms have been reported for different applications [18–20].

Among them, cobalt and iron Schiff base complexes have gained especially attention as synthetic models with the similarity of the iron-containing enzymes and cobalt-containing metallo-proteins [21, 22]. The Co(II)/Fe(III) metal complexes of tetradentate Schiff base ligands have been studied extensively in many fields such as catalysis for a variety of reactions including oxidation, epoxidation, hydroxylation,

polymerization [23, 24], biologically active reagents [25, 26] and synthetic dioxygen carriers by coordinating dioxygen reversibly [27]. However, the catalytic features of Schiff base Co(II)/Fe(III) metal complexes as cathode catalyst which may provide a cost effective approach have not been examined in microbial fuel cell (MFCs).

MFCs are novel biotechnological devices generating sustainable electricity from organic materials [28]. The MFC technology allows bioremediation of environmental contaminants including heavy metals, textile dyes, antibiotics, etc. [29–32]. In principle, electrogenic microorganisms utilize carbon sources, and electrons coming from the degradation of substrates are transferred to the anode surface, whereas protons are combined with oxygen producing water as cathode reaction [33]. Finding alternative and cost effective catalysts are very important for landfield and environmental applications of MFCs. Various catalysts such as reduced graphene oxide, tungsten oxide, xerogel and platinum were reported to be used in cathode preparation for MFC applications [34–37]. Cathodic Fe–N–C catalyst was reported using modified sacrificial support method (SSM) [38]. Cobalt nanoparticles nanopolyhedra electrocatalyst was reported via pyrolysis bimetallic metal–organic frameworks to be used in MFC technology [39]. However, metal complexes of Schiff base catalyst, which may provide a cost effective approach, have not been examined in MFCs.

In this study, a novel Schiff base which serves as two *N*,*O*-chelating was designed as target ligand for the first time, and examined as cathode catalysts in single chamber air cathode MFCs. The condensation reaction of an aromatic aldehyde derivative with 1,4-bis(3-aminopropyl) piperazine in a 2:1 ratio resulted in Schiff base structure containing diimine group. The synthesis and characterization of its cobalt (II) and iron (II) complexes containing piperazine core were performed. Piperazine is a well known building block as nitrogen-containing group which stabilizes the redox active metals to the higher oxidation states [40].

Prepared catalysts were employed in cathode preparation, and MFC performances were examined voltage generation and power density levels. The electrochemical and morphological features of cathode materials prepared using metal complexes of Schiff base were investigated, voltammetric and scanning electron microscopic techniques, respectively.

2 Experimental

2.1 Chemicals

4-Tert-butylphenol, 1,4-bis(3-aminopropyl)-piperazine, 2,6 lutidine, $SnCl_4$, paraformaldehid, toluene, dimethyl sulfoxide (DMSO), tetrahydrofuran (THF), ethanol, chloroform ($CHCl_3$), diethyether, calcium chloride, KOH, NaH, $Co(OAc)_2$, $FeCl_3{\cdot}6H_2O$ were obtained from Sigma-Aldrich. All solvents were dried and purified according to the procedures given by Perrin and Armarego before using [41]. Thin layer chromatography (TLC) based on silica gel 60-HF254 as an adsorbent was applied for monitoring the progress of the reactions. The synthesis of 5-*tert*-butyl-2-hydroxybenzaldehyde (**1**) was according to the reported procedure [42]. D-Glucose and sodium acetate trihydrate was from VWR (Karlsruhe, Germany). All other chemicals used in this study were analytical grade and obtained from commercial sources.

2.2 Instruments

Bruker ALPHA FT–IR spectrometer with universal attenuated total reflectance (ATR) sampling accessory was used for Infrared spectra. ^{1}H-NMR and ^{13}C-NMR spectra were analyzed using a Bruker AVANCE II 600 MHz NMR spectrometer with tetramethylsilane (TMS) as an internal reference. A Vario-Elementar Microcube ELIII was used for elemental analyses. Bruker AutoFLEX III Smart-beam TOF/TOF mass spectrometer was used for mass spectra analysis, and a-cyano-4-hydrocinnamic acid was used as the matrix. Absorption properties were analyzed using a spectrophotometer (Shimadzu UV-2550, Kyoto, Japan).

2.3 Synthesis

2.3.1 Synthesis of *N*,*N*′-bis[(3-tert-butyl-2-hydroxybenzylidene)-propyl]-piperazine (H_2L) (2)

The 1,4-bis(3-aminopropyl)-piperazine (0.562 g, 0.0028 mol) solution in ethanol (25 mL) was added drop wise to the solution of 5-*tert*-butyl-2-hydroxy-benzaldehyde (**1**) (1 g, 0.0056 mol) in ethanol (25 mL). The reaction mixture was degassed by argon at room temperature and the reaction mixture stirred under reflux for 6 h. The course of the reaction was monitored by TLC ($CHCl_3$/EtOH 10/0,1). After the reaction was completed, the solution cooled to room temperature was evaporated to 1/3 volume. The precipitated product was filtered off, washed with ethanol and diethyether, and dried. Yield: 82% (1.18 g). FT-IR (UATR-TWO™) ν_{max}/cm^{-1}: 3363 (OH), 3058, 3026 (Ar, C–H), 2950–2811 (Aliph., C–H), 1632 (C=N), 1589 (Ar, C=C), 1491–1361 (Aliph., C–C), 1267 (Ar–O–H), 1156, 1049, 823, 751. ^{1}H–NMR ($CHCl_3$) δ (ppm): 13.41 (s, 2H), 8.36 (s, 2H), 7.36 (d, 2H), 7.23 (d, 2H), 6.91 (d, 2H), 4.76 (s, 2H), 3.63 (t, 4H), 3.47 (s, 2H), 2.44 (t, 8H), 1.92–1.87 (m, 4H), 1.31 (s, 18H). ^{13}C-NMR ($CHCl_3$) δ (ppm): 165.34, 158.94, 141.16, 129.50, 127.56, 118.01, 116.55, 57.65, 56.03, 53.17, 33.99, 31.48, 28.01. UV–Vis (DMSO): λ_{max} (nm) (log ε) 261 (4.09), 321 (3.75). MS (MALDI-TOF): m/z 522.02 $[M+1]^+$.

2.4 Synthesis of Cobalt (II) Complex (3)

In a 100 mL round bottom flask, a solution of KOH (107.5 mg, 1.92 mmol) in ethanol (10 mL) was added to the stirred solution of H_2L (**1**) (500 mg, 0.96 mmol) and degassed with argon at room temperature. After the mixture was stirred for 15 min, anhydrous $Co(OAc)_2$ (170 mg, 0.96 mmol) was added to the reaction mixture under inert atmosphere. The mixture was heated to reflux during 6 h and then it was cool down. The solution was concentrated and the formed complex was filtered off. The collected product was washed with ethanol and dried in desiccators over anhydrous calcium chloride under vacuum. Yield: 58% (321 mg). FT-IR (UATR-TWO™) ν_{max}/cm^{-1}: 3021 (Ar, C–H), 2951–2810 (Aliph., C–H), 1621 (C=N), 1534 (Ar, C=C), 1474–1362 (Aliph., C–C), 1272 (Ar–O), 1172, 1113, 835. UV–Vis (DMSO): λ_{max} (nm) (log ε) 262 (4.31), 401 (3.50). MS (MALDI-TOF): m/z 577.86 $[M]^+$.

2.5 Synthesis of Iron (III) Complex (4)

The suspension of NaH (46.1 mg, 1.92 mmol) in THF at °C was added to the stirred solution of H_2L (**1**) (500 mg, 0.96 mmol). After the evolution of gas has discontinued, the mixture was stirred at reflux temperature for 2 h. After the solution was cooled down, $FeCl_3{\cdot}6H_2O$ (260 mg, 0.96 mmol) was introduced and reflux was continued for further 4 h. The complex was precipitated by adding brine solution and the formed product was separated from the solution by filtration. The collected product was washed with ethanol and dried in desiccators over anhydrous calcium chloride under vacuum. Yield: 82% (1.18 g). FT-IR (UATR-TWO™) ν_{max}/cm^{-1}: 3055 (Ar, C–H), 2953–2856 (Aliph., C–H), 1620 (C=N), 1539 (Ar, C=C), 1479–1361 (Aliph., C–C), 1269 (Ar–O), 1144, 1107, 837. MS (MALDI-TOF): m/z 574.84 $[M–Cl]^+$. UV–Vis (DMSO): λ_{max} (nm) (log ε) 264 (3.79), 328 (3.41), 420 nm (3.19).

2.6 MFC Construction and Preparation of Cathode Using the Complexes

Single chamber air–cathode MFCs with working volume of 12 mL were prepared according to a previous paper [43]. Anode was prepared using a commercial carbon cloth (Lot: 14032102, FuelCells, Texas, 7 cm^2). Air cathode was also prepared using carbon cloth (CTO32414, FuelCells, Texas, 7 cm^2) according to a previous paper with modifications [44]. Carbon/poly(tetrafluoroethylene) (PTFE) was applied onto the air facing side of the cathode. The following catalyst mixtures were spread onto the surface of cathode using Nafion perfluorinated solution (CAS. No: 31175, Sigma-Aldrich): (i) control cathode with only activated carbon powder (1 mg cm^{-2} cathode area); (ii) Cobalt complex-cathode containing 1 mg cm^{-2} Co-complex mixed with activated carbon; (iii) Fe-complex containing 1 mg cm^{-2} Fe-complex mixed with activated carbon.

2.7 MFC Operations

A bacterial inoculum enriched from local wastewater treatment plant (Pasakoy Advanced Biological Wastewater Treatment Plant, Istanbul, Turkey) was used during MFC operations. Glucose (1.2 g L^{-1}) was used as the carbon source in each MFC with a medium solution containing: NH_4Cl (0.31 g L^{-1}); $NaH_2PO_4{\cdot}H_2O$ (5.84 g L^{-1}); $Na_2HPO_4{\cdot}7H_2O$ (15.47 g L^{-1}); KCl (0.13 g L^{-1}), a mineral solution (12.5 mL) and a vitamin solution (12.5 mL) as reported previously [45]. The medium was refreshed when the voltage dropped below 50 mV. All experiments were repeated twice. The MFC operations were carried out in a temperature controlled room 32 ± 2 °C).

2.8 Calculations and Analysis

A data acquisition system (ADC24, Picolog; Cambridgeshire, UK) was used to monitor voltage generation by the MFCs.

The following equation was used to calculate power density (mW/m^2);

$$P = IV/A, \quad (1)$$

where P is the power density, I is the current, V is the voltage and A is the surface area of the electrode (7 cm^2). All experiments were repeated twice (n = 2).

The cyclic voltammetry (CV) test was applied for the samples control, Co-complex, and Fe-complex for 9 cycles each from 0.2 to − 0.6 V Vs Ag/AgCl using a potentiostat system (Parstat MC, Ametek, Oak Ridge, Tennessee). The measurements were performed in the solution of 100 mM Na_3PO_4 while nitrogen was purging in the cell. The area was set to be 1 cm^2 and the samples are glued to a Pt plate electrode as working electrode using 12660-Graphite, isopropanol base (EMS diasum) and the counter electrode was a Pt plate with the same area. The cathode surfaces were analyzed using a scanning electron microscope (FESEM, LEO Supra VP-55, Zeiss, Germany) coupled with Oxford X-max N Energy Dispersive X-Ray Spectroscopy system.

3 Results and Discussion

3.1 Synthesis and Characterization

The 5-*tert*-butyl-2-hydroxy benzaldehyde (**1**) compound was obtained from the reaction of $SnCl_4$ and paraformaldehyde in the presence of 2,6 lutidine in toluene by applying the

literature procedure to obtain aldehyde functional group in the *ortho*-position of aromatic phenols [42]. The new ligand (**2**) containing bis-imine as *N*,*O*-chelating was prepared by the usual condensation reaction of the aldehyde derivative (**1**) and 1,4-bis(3-aminopropyl)piperazine in anhydrous ethanol at reflux temperature. The complexation reactions of H_2L **(2)** was carried out with $Co(OAc)_2$ for **3** and $FeCl_3{\cdot}6H_2O$ for **4** in ethanol under basic conditions (Scheme 1).

The common spectroscopic methods such as FT-IR, ^{1}H-NMR, ^{13}C-NMR, UV/Vis and MS and elemental analysis were employed for the characterization of achieved compounds. The results obtained confirmed the expected structures.

The FT-IR spectrum of **2** showed the imine vibration band at 1632 cm^{-1} with the disappearance of the aldehyde peak at 1627 cm^{-1} resulting from compound **1** as a proof of the condensation reaction to give Schiff base. The typical O–H vibration was observed at 3363 cm^{-1} in the FT-IR spectrum of **2**. The typically Ar–OH vibrations were observed at 1267 cm^{-1} and 1049 cm^{-1} as asymmetrical and symmetrical vibrational bands for compound **2**. The aliphatic C–H bands belonging to the $–CH_3$ groups on the benzene ring and $–CH_2$ groups originating from piperazine were seen at between 2950 and 2811 cm^{-1}. The FT-IR spectra of the complexes (**3,4**), the most significant differences were that the imine (C=N) and Ar–O– vibrations shifted to 1621 cm^{-1} and 1272 cm^{-1} for **3**, 1620 cm^{-1} and 1269 cm^{-1} for **4** upon complexation with cobalt and iron. The aliphatic C–H bands were observed at between at 2951–2810 cm^{-1} for compound **3**, at 2953–2856 cm^{-1} for compound **4**.

When compared the ^{1}H-NMR spectra of compound **1** and **2**, the disappearances of HC=O proton signal of **1** and the appearance of CH=N proton at 8.36 ppm shows that the imine condensation reaction carried out. In addition to this, in the ^{1}H-NMR spectrum of **2**, phenolic OH protons revealed at 13.41 ppm due to hydrogen bonding between imine and OH group. The methylene protons were observed at between 4.76 and 1.87 ppm. The methyl protons on benzene ring were appeared at 1.31 ppm as singlet.

When the obtained ^{13}C-NMR is evaluated, the peak at 165.34 ppm belonging to the imine carbon atom group is the characteristic proof for the Schiff base formation for compound (**2**). The aromatic and aliphatic carbon peaks were observed at between 158.94 and 116.55 ppm and 57.65–28.01 ppm, respectively.

The mass spectra were gained for all new compounds (**2**–**4**) by utilizing MALDI-TOF mass spectrometer and confirmed the proposed structures. The expected molecular ion peaks of all compounds (**2**–**4**) were obtained at m/z 522.02 $[M+1]^+$ for **2**, m/z 577.86 $[M]^+$ for **3** and m/z 574.84 $[M–Cl]^+$ for **4**, as seen in Fig. 1.

The electronic absorption spectra of the prepared ligand (**2**) and its cobalt (**3**) and iron complex (**4**) were examined in 1×10^{-4} M concentration of DMSO solution for comparison purposes as shown in Fig. 2. In the electronic spectra of free Schiff base ligand (**2**), the bands at 261 nm and 321 nm are attributed to π–π* and n–π* transitions [46]. The electronic spectra of the complex **3** in DMSO displayed a single d–d transition at 262 nm and a charge-transfer transition at 401 nm. The appearance of a single d–d transition in DMSO is attributed to the effect of coordination of solvent which forms low-spin six-coordinate distorted octahedral [21]. In the absorption spectrum of complex **4** taken in DMSO, the electronic transitions for iron(III) systems are spin forbidden and hence weak [47]. The higher intensity band below 320 nm is of ligand origin assignable to intraligand n–π*/π–π* transition. The broad and weak resolved band at 420 nm may be assigned to LMCT or MLCT [48].

3.2 MFC Performance Results

Figure 3 shows voltage generation results using cathode materials prepared with Co and Fe Schiff base catalysts and control in single chamber air cathode MFCs. The voltage reached up to 0.35 V when Fe-Schiff base catalyst used during operations while control cathode having only activated carbon generated around 0.3 V at external resistance of 980 Ω.

Power density results showed that Fe-Schiff base catalyst generated higher power density levels of 142 mW m^{-2} at the current density of 0.08 mA cm^{-2} (Fig. 4). Co-Schiff base generated the lowest maximum power density of 85 mW m^{-2} at the current density of 0.06 mA cm^{-2} when compared to the control and Fe-Schiff base catalyst. The voltage was decreased down to 0.2 V when the cathode is replaced with Co-Schiff base. These results indicate that Fe-Schiff base might be good candidate for electricity production in MFCs. Cobalt complexes can bind oxygen better when compared to iron complexes [22]. Since air cathode was used in this study, a lower voltage generation by cobalt complex may be resulted because of limited oxygen diffusion into the MFC due to higher oxygen absorption by the cobalt complex when compared to the iron complex. Another important point is that cobalt may be more toxic element when compared to iron which would affect the microbial flora not only on the surface of cathode, but also in the whole microbial dynamics in MFCs. The incorporation of metals into polymeric materials may show antibacterial properties [49]. Although current density achieved using platinum catalyst on the cathode is higher when compared to Co–Fe Schiff bases (0.78 mA cm^{-2}) [33], the current density values are in expected ranges. However, since the cathode catalysts developed and examined in this study are quite cost effective when compared to the platinum, the technology can be integrated into wastewater treatment plants.

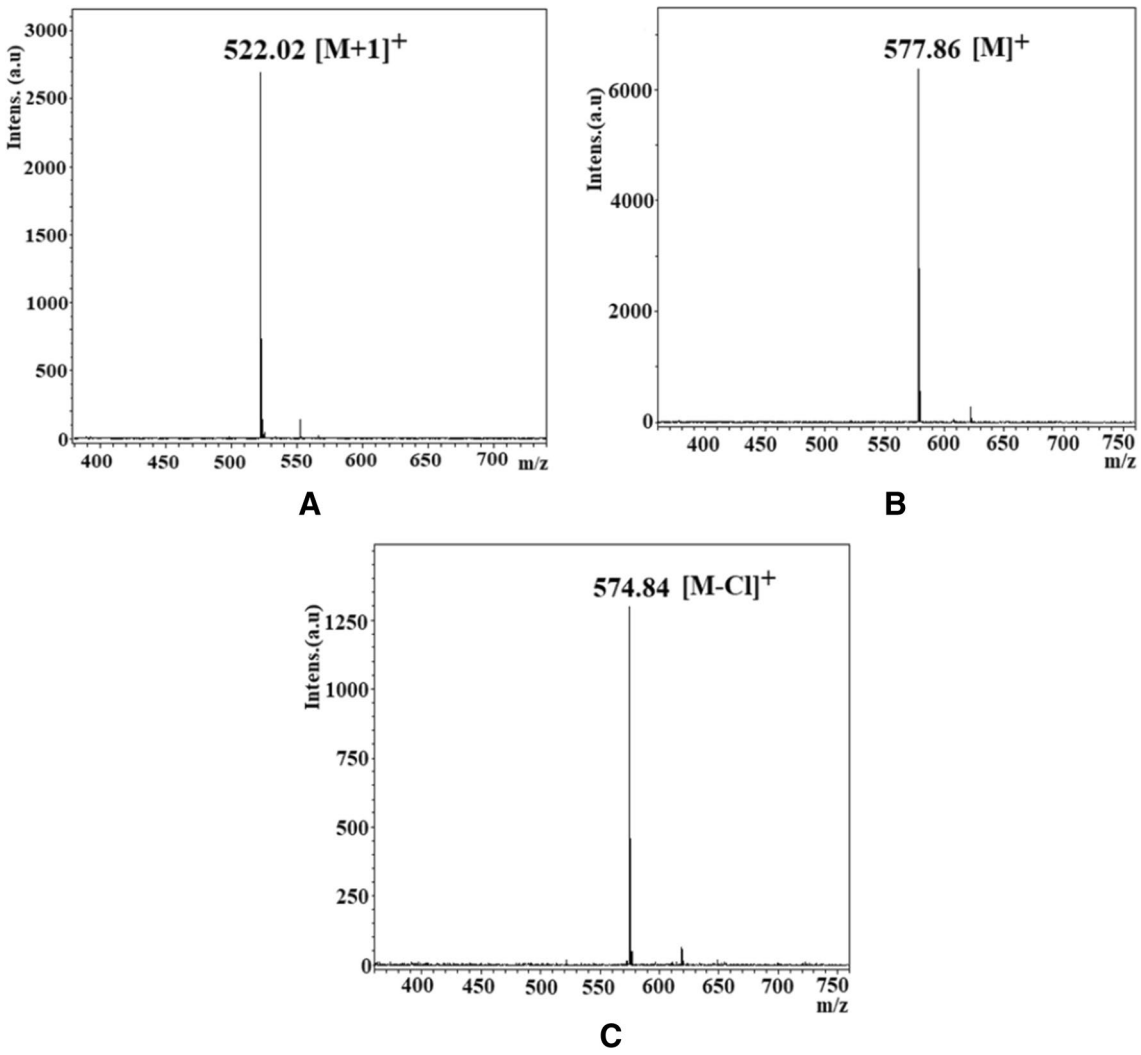

Fig. 1 MALDI-TOF MS spectra of **2** (**a**), **3** (**b**) and **4** (**c**)

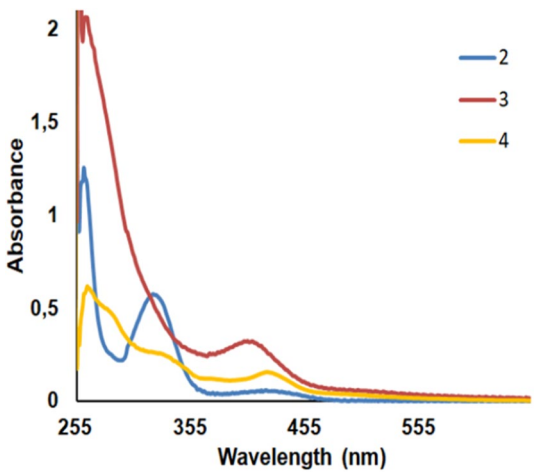

Fig. 2 Electronic absorption spectra of the H_2L (**2**) and complexes (**3,4**) in DMSO (Concentration 1×10^{-4} mol L^{-1})

In general, platinum catalysts are commonly used in MFC operations generating higher power density values. However, Fe-Schiff base catalysts might be alternative for platinum catalysts with their cheaper and cost effective preparation procedures. Moreover, novel nanotechnological approaches can be applied in order to improve the efficiency of Fe-Schiff base catalysts.

Figure 5 shows cyclic voltammograms, recorded at room temperature in substrate-limiting culture medium at the same scan rate. The background current in Fe-Schiff base complex is lower when compared to the control cathode while Co-Schiff base complex showed a higher background current. These results confirmed voltage generation results obtained during MFC operations.

Scanning electron microscopic images showed the surfaces of cathodes examined as water facing side of the cathodes (Fig. 6). Energy dispersive X-ray spectroscopy results showed the elemental distribution on the cathode surfaces

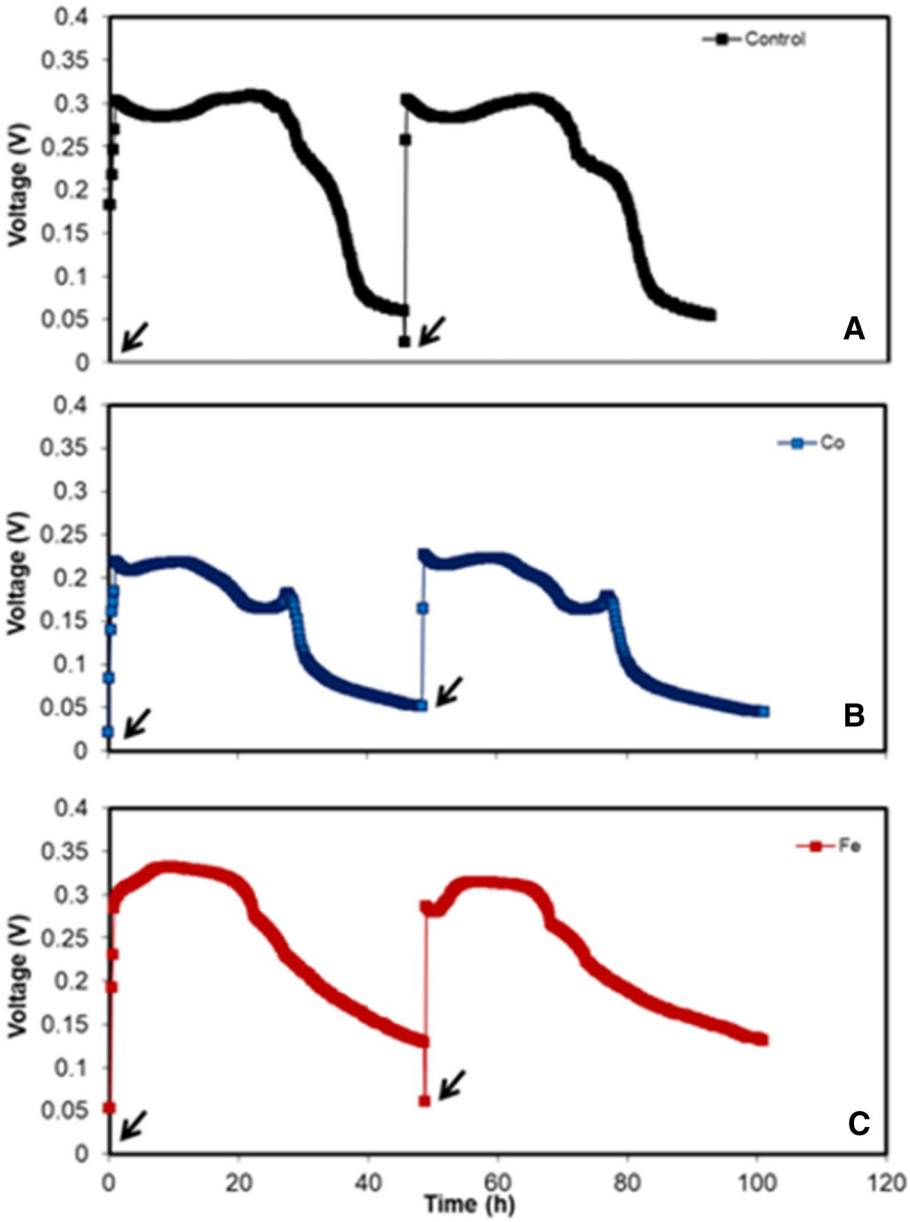

Fig. 3 Voltage generation using novel complex catalysts in single chamber MFC. External resistance is 980 Ω

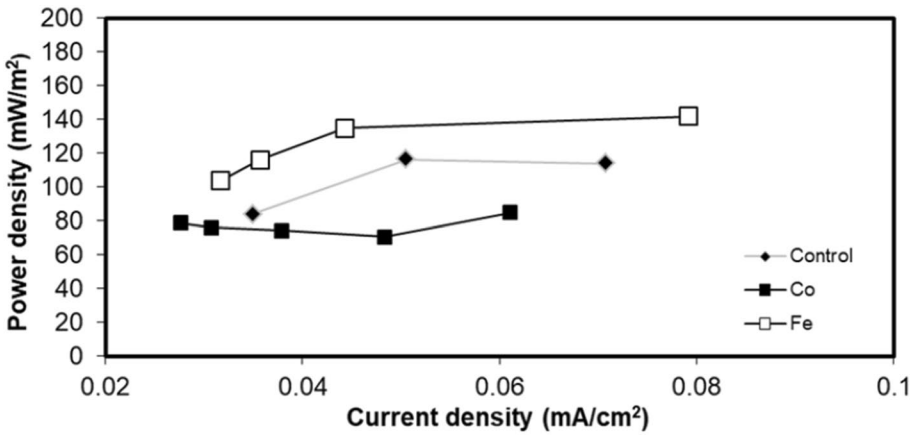

Fig. 4 Power density results of the Schiff base Co and Fe complexes used as cathode catalysts in single chamber MFCs

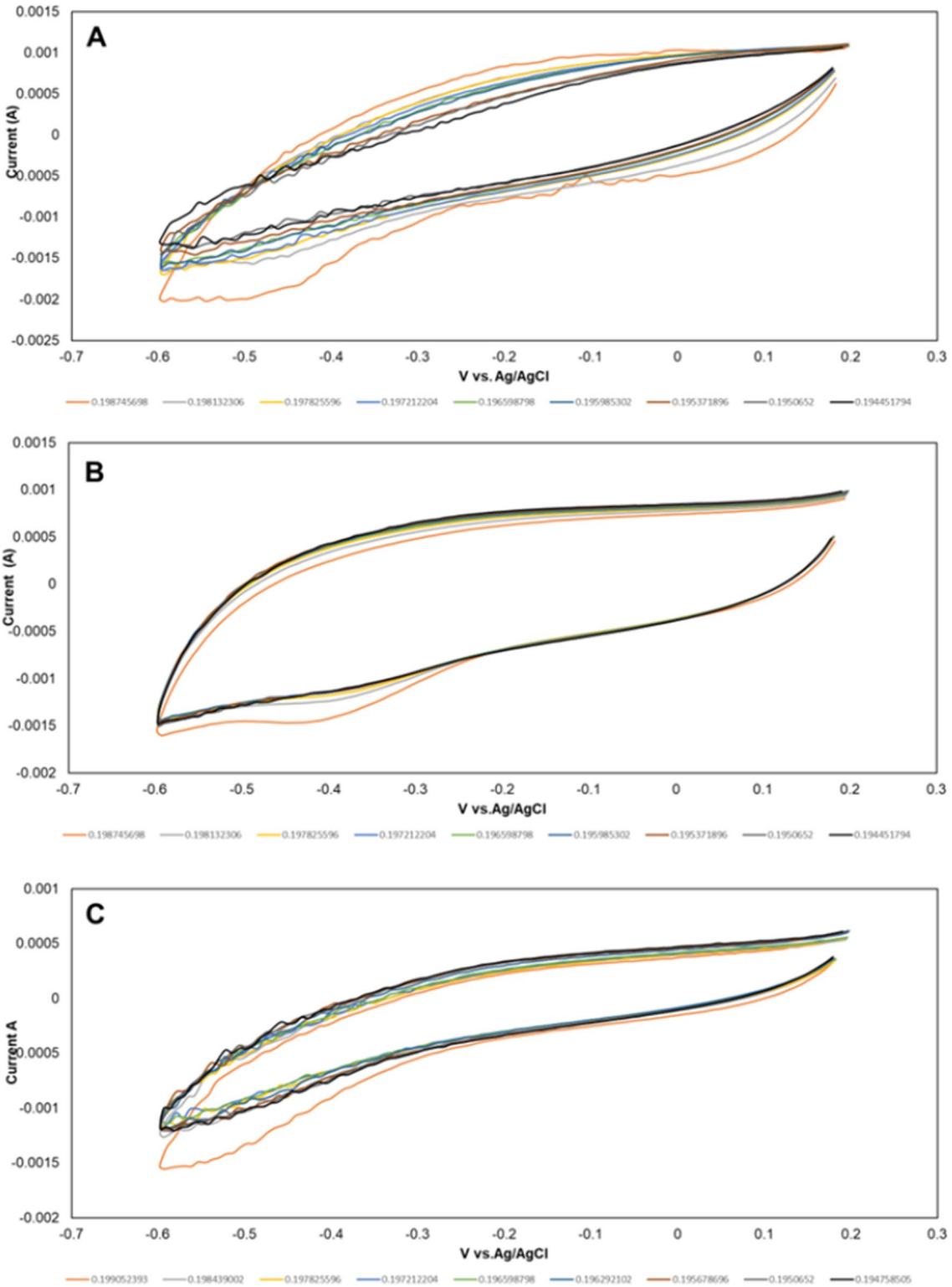

Fig. 5 Cyclic voltammograms of the cathode materials, recorded at room temperature in substrate-limiting culture medium at the same scan rates. **a** control; **b** Co-complex; **c** Fe-complex

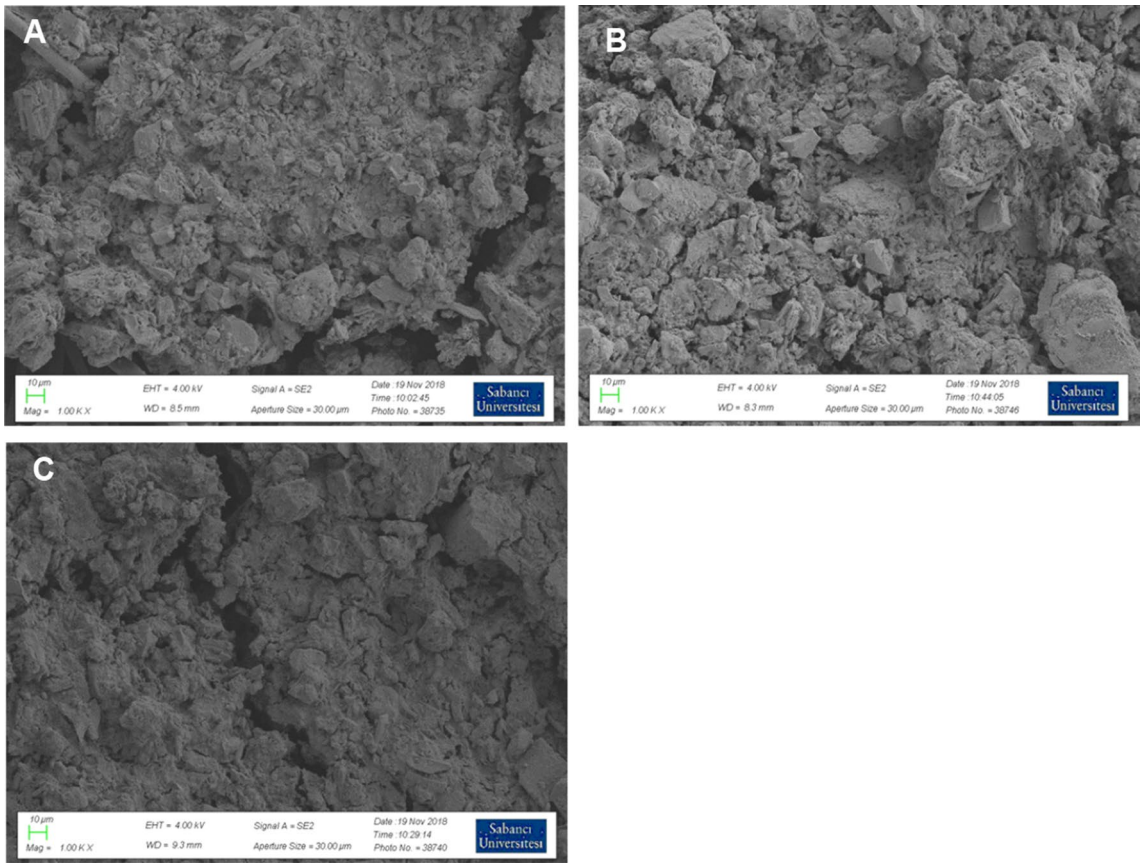

Fig. 6 SEM images of control (**a**), Co (**b**) and Fe (**c**) complex catalyst coated on water facing side of the cathodes

(Fig. 7). Our results indicate that Fe and Co-Schiff base catalysts can be bind to the surface of cathodes to be used in MFCs. Although biofouling on the cathode surface may affect MFC performance [50], bacterial accumulation over time during operations may decrease oxygen diffusion into the chamber which may increase Coulombic efficiency. And, although nanostructures are preferred on the surface of cathodes, the surfaces of the cathodes developed in this study also show microstructures.

Recent efforts have been focusing of finding alternative cost effective catalysts for MFC cathodes. The cathodes prepared using novel Co and Fe complexes of Schiff base as demonstrated in this study provide alternative technique for MFC applications. While platinum is commonly used in MFCs, Schiff base metal complexes can also employed especially for wastewater treatment plants in order to recover energy from wastes. And, the approach shown here may also decrease the MFC operating cost.

4 Conclusion

In conclusion, novel Co and Fe—Schiff base catalysts were synthesized, and used as cathode catalysts in MFCs. Spectroscopic results such as ^{1}H-NMR, ^{13}C-NMR, FT-IR, UV–Vis and MS and elemental analysis confirmed the structural findings. MFC results show that Fe-Schiff base complex would be better when compared to Co-Schiff base complex and control cathodes indicating that the Fe-complex can be employed into MFCs for land field applications for renewable and green energy generation for a better climate and cleaner environment.

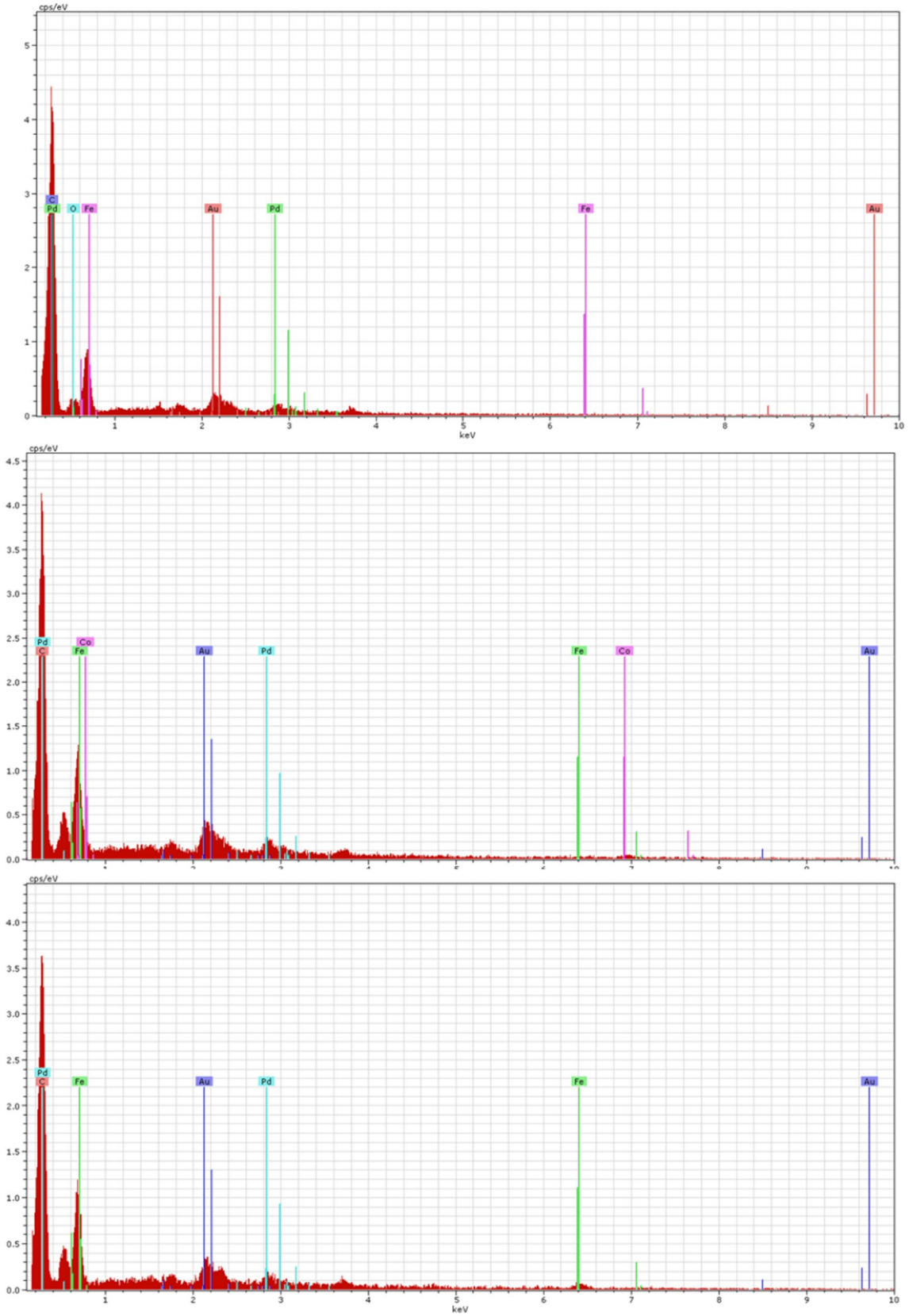

Fig. 7 Energy dispersive X-ray spectroscopy result of the cathode surfaces of control (**a**), Co-complex of Schiff base (**b**) and Fe-complex of Schiff base (**c**)

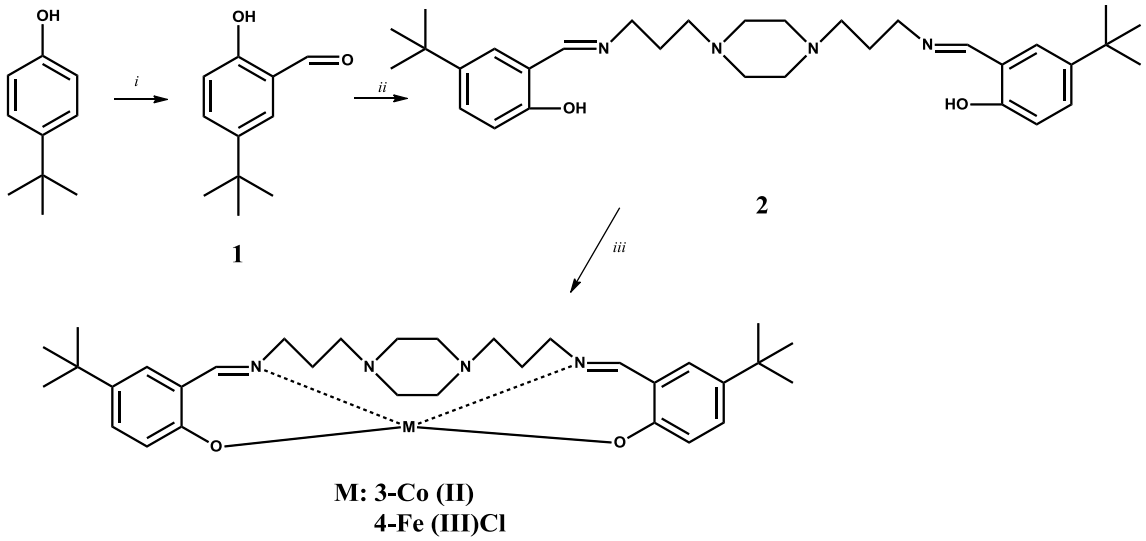

Scheme 1 Synthesis route: (i) $SnCl_4$, 2,6 lutidine, paraformaldehyde, toluene (ii) 1,4-bis(3-aminopropyl) piperazine, ethanol, reflux temperature (iii) KOH, $Co(OAc)_2$, ethanol, reflux temperature for **3**, NaH, THF, $FeCl_3$ for **4**, from °C to reflux temperature

Compliance with Ethical Standards

Conflict of interest There are no competing interests to declare.

References

1. E. Sinn, C.M. Harris, Coordin. Chem. Rev. **4**, 391 (1969)
2. G.I. Dzhardimalieva, I.E. Uflyand, J. Inorg. Organomet. Polym. **28**, 1305 (2018)
3. A. Prakash, D. Adhikari, Int. J. ChemTech Res. **3**, 1891 (2011)
4. W. Qin, S. Long, M. Panunzio, S. Biondi, Molecules **18**, 12264 (2013)
5. E. Yousif, A. Majeed, K. Al-Sammarrae, N. Salih, J. Salimon, B. Abdullah, Arab. J. Chem. **10**, 1639 (2017)
6. H.S. Abbo, S.J.J. Titinchi, Appl. Catal. A **435–436**, 148–155 (2012)
7. N.S. Venkataramanan, G. Kuppuraj, S. Rajagopal, Coord. Chem. Rev. **249**, 1249–1268 (2005)
8. K. Shanker, R. Rohini, V. Ravinder, P.M. Reddy, Y. Ho, Spectrochim. Acta Part A **73**, 205–211 (2009)
9. D.A. Atwood, J.A. Jegier, D. Rutherford, Inorg. Chem. **35**(35), 63–70 (1996)
10. S. Sobha, R. Mahalakshmi, N. Raman, Spectrochim. Acta Part A **92**, 175–183 (2012)
11. K.C. Gupta, A.K. Sutar, Coord. Chem. Rev. **252**, 1420 (2008)
12. C.W. Tang, S.A. VanSlyke, Appl. Phys. Lett. **51**, 913 (1987)
13. A.W. Jeevadason, K.K. Murugavel, M.A. Neelakantan, Renew. Sustain. Energy Rev. **36**, 220 (2014)
14. M.S. Iqbal, A.H. Khan, B.A. Loothar, I.H. Bukhari, Med. Chem. Res. **18**, 31 (2009)
15. C.M. da Silva, D.L. da Silva, L.V. Modolo, R.B. Alves, M.A. de Resende, C.V.B. Martins, A. de Fatima, J. Adv. Res. **2**, 1 (2011)
16. S.D. Bella, Chem. Soc. Rev. **30**, 355 (2001)
17. S. Yamada, Coord. Chem. Rev. **190–192**, 537 (1999)
18. J. Tong, Y. Zhang, Z. Li, C. Xia, J. Mol. Catal. A **249**, 47 (2006)
19. A.H. Kianfar, L. Keramat, M. Dostani, M. Shamsipur, M. Roushani, F. Nikpour, Spectrochim. Acta Part A **77**, 424 (2010)
20. C.R. Bhattacharjee, C. Datta, G. Das, P. Mondal, Mater. Sci. Eng. C **32**, 735 (2012)
21. V.K. Sivasubramanian, M. Ganesan, S. Rajagopal, R. Ramaraj, J. Org. Chem. **67**, 1506 (2002)
22. A. Blgotto, G. Costa, G. Mestroni, G. Pellizer, A. Puxeddu, E. Reisenhofer, L. Stetanl, G. Tauzher, Inorg. Chim. Acta Rev. **4**, 41 (1970)
23. S. Forster, A. Rieker, J. Org. Chem. **61**, 3320 (1996)
24. H.S. Abbob, S.J.J. Titinchic, R. Prasada, S. Chand, J. Mol. Catal. A **225**, 225 (2005)
25. L.A. Saghatforoush, A. Aminkhani, F. Chalabian, Transition Met. Chem. **34**, 899 (2009)
26. A.A. Nejo, G.A. Kolawole, A.O. Nejo, J. Coord. Chem. **63**, 4398 (2010)
27. G.Q. Li, R. Govind, Ind. Eng. Chem. Res. **33**, 755 (1994)
28. T. Catal, A. Kul, V. Enisoglu-Atalay, H. Bermek, S. Ozilhan, N. Tarhan, J. Power Sources **414**, 1 (2019)
29. M. Ozdemir, V. Enisoglu-Atalay, H. Bermek, S. Ozilhan, N. Tarhan, T. Catal, Bioresour. Technol. Rep. **5**, 121 (2019)
30. T. Catal, S. Yavaser, V. Atalay, H. Bermek, Bioresour. Technol. **268**, 116 (2018)
31. M. Kumru, H. Eren, T. Catal, A.T. Akarsubaşı, H. Bermek, Environ. Technol. **33**(16–18), 2167 (2012)
32. C. Abourached, T. Catal, H. Liu, Water Res. **51**, 228 (2014)
33. T. Catal, S. Xu, K. Li, H. Bermek, H. Liu, Biosens. Bioelectron. **24**, 849 (2008)
34. G. Massaglia, I. Fiorello, A. Sacco, V. Margaria, C.F. Pirri, M. Quaglio, Nanomaterials **9**, E36 (2018)
35. Y. Wu, L. Wang, M. Jin, F. Kong, H. Qi, J. Nan, Bioresour. Technol. **283**, 129 (2019)
36. S. Das, M.M. Ghangrekar, Environ. Technol. **25**, 1 (2019)
37. B.S. Thapa, S. Seetharaman, R. Chetty, T.S. Chandra, Enzyme Microb. Technol. **124**, 1 (2019)

38. C. Santoro, M. Kodali, N. Shamoon, A. Serov, F. Soavi, I. Merino-Jimenez, I. Gajda, J. Greenman, I. Ieropoulos, P. Atanassov, J. Power Sources **412**, 416 (2019)
39. S. Zhang, W. Su, X. Wang, K. Li, Y. Li, Biosens. Bioelectron. **127**, 181 (2019)
40. T. Sehwenkmis, A. Berkeasel, Tetrahedron Lett. **34**, 4785 (1993)
41. D.D. Perrin, W.L.F. Armarego, D.R. Perrin, *Purification of Laboratory Chemicals* (Pergamon Press, New York, 2013)
42. S. Jammi, L. Rout, T. Punniyamurthy, Tetrahedron **18**, 2016 (2007)
43. H. Bermek, T. Catal, S.S. Akan, M.S. Ulutaş, M. Kumru, M. Özgüven, H. Liu, B. Özçelik, A.T. Akarsubaşı, World J. Microbiol. Biotechnol. **30**, 1177 (2013)
44. S. Cheng, H. Liu, B.E. Logan, Electrochem. Commun. **8**, 489 (2006)
45. D.R. Lovley, E.J.P. Phillips, Appl. Environ. Microbiol. **54**, 1472 (1988)
46. R.L. Carlin, J. Chem. Educ. **46**, A628 (1969)
47. F. Shabani, L.A. Saghatforoush, S. Ghammamy, Bull. Chem. Soc. Ethiop. **24**, 193 (2010)
48. Y. Maeda, N. Tsutsumi, Y. Takashima, Inorg. Chem. **23**, 2441 (1984)
49. F. Zafar, H. Zafar, E. Sharmin et al., J. Inorg. Organomet. Polym. **21**, 646 (2011)
50. M.T. Noori, M.M. Ghangrekar, C.K. Mukherjee, B. Min, Biotechnol. Adv. **22**, 107420 (2019)